Arab J Geosci (2016) 9:435
DOI 10.1007/s12517-016-2466-y

ORIGINAL PAPER

Integrated application of geoelectrical techniques for structural investigations: case study of Wadi Marsad Graben, Jordan

Mahmoud M. El-Waheidi[1] · **Habes A. Ghrefat**[1] · **Awni Batayneh**[2] · **Yousef H. Nazzal**[3] · **Taisser Zumlot**[1]

Received: 12 July 2015 / Accepted: 7 April 2016

Abstract An integrated geoelectrical survey has been conducted at the Wadi Marsad area, south of Jordan, to map the dominant structural features associated with the Arabian-African plate movements. The area is known to be tectonically affected by the epeirogenic movements of the Arabian shield which originated several major and minor structural features. Fifty-four vertical electrical soundings (VES) using Schlumberger configuration and nine induced polarization (IP) profiles (both resistivity and metal factor parameters were determined) were carried out in the investigated area. The integrated use of IP and VES surveys has proved to be efficient in mapping the lateral and vertical extensions of a major graben structure existing in the investigated area.

✉ Mahmoud M. El-Waheidi
melwaheidi@ksu.edu.sa

Habes A. Ghrefat
habes@ksu.edu.sa

Awni Batayneh
awni_batayneh@yahoo.com

Yousef H. Nazzal
yousef.nazal@gmail.com

Taisser Zumlot
tzumlot@ksu.edu.sa

[1] Geology and Geophysics Department, Science College, King Saud University, P.O. Box 2455, Riyadh 11451, Kingdom of Saudi Arabia

[2] Department of Earth and Environmental Sciences, Yarmouk University, Irbid 21163, Jordan

[3] Department of Applied Mathematics and Sciences, College of Arts & Sciences, Abu Dhabi University, Post Box 59911, Abu Dhabi, UAE

Keywords Induced polarization · Vertical electrical sounding · Resistivity · Graben

Introduction

The integrated application of geophysical methods applied for structural and tectonic studies is a common procedure used to overcome the lack of direct geological information about the investigated subsurface structures (Simiyu and Keller 1997; Adepelumi et al. 2006; Nicolas and Keller 2007). The investigated area is located south of Jordan, as shown in Fig. 1a. It makes part of the Arabian-African pre-Cambrian shield that is mainly composed of basement rocks. The pulsated up and down movements of the shield during the epeirogenic activities represent the major tectonic factor affected in the geologic history of the area. These epeirogenic movements resulted in marine transgressions and regressions causing the deposition of considerable thickness of sediments.

The geoelectrical survey carried out in the area included vertical electrical sounding (VES) measurements conducted using the Schlumberger configuration and induced polarization (IP) profiles using dipole-dipole array. The purpose of the study is to map the major structural features present in the area and also to apply geophysical methods to constrain the structural configuration of the area.

Geological Setting

The geological succession in Wadi Marsad, as shown in Fig. 1b, starts with the surface Quaternary deposits (youngest). This geological succession mainly composed of alluvial and wadi sediments, alluvium sand, and mud flats of pelitic

Published online: 14 May 2016

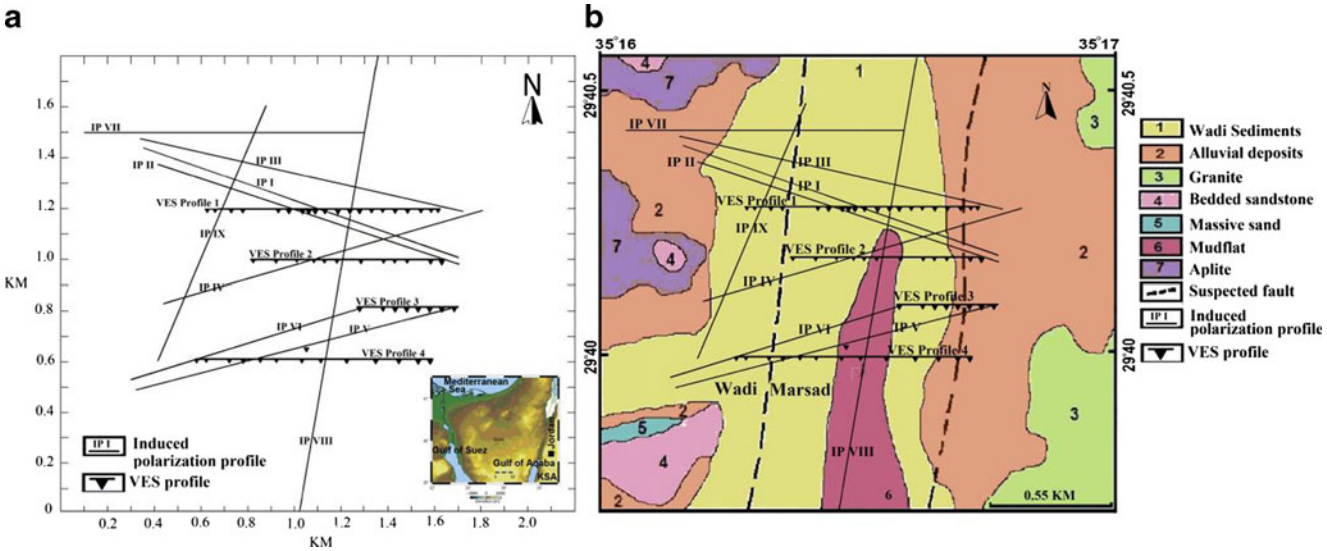

Fig. 1 **a** Location map of geoelectrical measurements. The *inset map* shows the regional location of the investigated area. **b** Geological map of Wadi Marsad

sediments. The thickness of these sediments reaches up to a few meters (Abdelhamid 1990).

The second part of the geological succession is Rum formation. It is composed of continental sandstone and reaches up to 1 km of thickness (Bender 1974). The formation is divided into several sandy groups that are differentiated from each other by their age and grain size. In general, the formation starts with a series that consists of up to 60 m of coarse to medium grain-bedded sandstone. The grain size of the series reaches up to 0.5 m (basal conglomerate) at the bottom while it has a medium size at the top.

The second series of the formation is composed of coarse-grained sandstone characterized by the absence of the basal conglomerate. The thickness of the series reaches 200 m. The last series of the Rum formation is composed of coarse-grained, massive sandstone with a less friable upper part, compared to the overlying series. Its maximum thickness is about 300 m.

The basement rocks of the pre-Cambrian age form the end of the geological succession in the Wadi Marsad area. These are mainly composed of granodiorite, granites, and metamorphic rocks with minor acidic and basic intrusive dikes. Structurally, the investigated area is located about 30 km ENE of the Gulf of Aqaba, close to the Arabia-Dead sea rift zone. This rift represents the continuation of the major rift structure recognizable from east of Africa to south of Turkey. Locally, several faults and lineaments are present in the area (Bender 1974).

Figure 1a, b depicts the regional location and geological map of Wadi Marsad Graben, Jordan. It further represents the structures and age of lithostratigraphic units of the Wadi Marsad area. "Lithostratigraphy" is the term which is used for describing the temporal and spatial relationships between the units of rocks. Understanding of such relationships appears to be essential so as to develop adequate and effective geologic history. It is due to the fact that lithostratigraphy determines structural complexity, large range of volcanic conditions, huge variety of rock types, intrusive environments, multiplicity of metamorphic events, and sedimentary, particularly intimidating within the Arabian shield. The lithostratigraphy is considered as the constant process which assists in advancing the degrees of reliability and refinement within concert, along with developments in information related to formation ages and origins of the rocks. Furthermore, lithostratigraphy assists in gathering adequate information related to metamorphic and structural modifications of the area.

The geoelectrical survey

The geoelectrical measurements conducted in the area included VES measurements and IP profiles. The measurements were carried out using the multipurpose multichannel GDP16 from Zonge Engineering & Research Organization, Inc. Location of all geoelectrical measurements are shown in Fig. 1.

In total, 54 VES stations using Schlumberger array have been conducted. These are grouped to form four geoelectric cross sections. The direction was chosen to be perpendicular (i.e. normal) to the regional trend of the strike within the area. The maximum current electrodes separation ranges from 500 to 1400 m. IP measurements were collected along nine profiles with the help of the inclusion of dipole-dipole array, having a dipole distance of 200 m. Both resistivity and metal factor (MF) parameters were measured. The frequencies utilized for the calculation of the metal factor were 0.3 and 3 Hz.

In the IP work, the measured parameters could be made either in frequency domain or in time domain. The most

common measured parameter has found to be the chargeability in the time domain. In the current study, the frequency domain, using an alternating current, is used to measure the IP effects by determining the resistivity at two different frequencies. There are mainly two ways to measure the IP effects in the frequency domain; specifically, the percentage frequency effect (PFE) and the metal factor (MF). In particular, the metal factor, defined by Eq. 1, has been utilized in order to analyze its response in the presence of structural features and to draw out useful conclusions. This parameter has been suggested by Marshall and Madden (1959) to correct for the variations of IP effect with effective resistivity of the host rock, that is, the type of electrolyte, temperature, and the size of pore.

$$\mathrm{MF} = 2\pi 10^5((p_{a0}-p_{a1})/(p_{a0}p_{a1})) \quad (1)$$

where p_{a0} is the apparent resistivity at low frequency and p_{a1} is the apparent resistivity at high frequency. The numerical multiplying factor in Eq. 1 is used to place the metal factor in the same numerical order as resistivity and chargeability (Sumner 1976). The field procedure for taking IP measurements is based on making gradual increase in the separating distance among the potential dipole and the current dipole in order to increase the penetration's depth permitting the logging of the electrical characteristics of the earth at several levels of depth. For each depth level (at fixed specific separating distance between both dipoles), the dipoles were moved along the whole length of the profile; this procedure allows making IP measurements at various depth levels within the required lateral extension.

VES data

Data processing

The first step in data processing was to calculate the apparent resistivities of the symmetrical Schlumberger configuration. The representation of the calculated apparent resistivity values was done on a bilogarithmic paper, where the half current electrode distances were plotted on the *x*-axis and the apparent resistivity values are plotted on the *y*-axis. Next, a filtering process was applied using a filter consists with 6-equidistant coefficients per decade. The scope of this process was to eliminate the disturbing oscillations resulted due to noise on the measuring values (Ghosh 1971). The used filter has the following coefficients: 0.008, −0.147, 0.0326, −0.01078, 1.1606, and −0.0984. The filtering process produced sounding curves less affected by noise and easier to be interpreted. A typical sounding curve obtained in the area with the best fit 1-dimensional model is shown in Fig. 2.

Qualitative interpretation of VES data

Due to the lack of direct geological information (borehole data) in the area, it was necessary to adopt an efficient method of qualitative interpretation. For this purpose, the association factor technique of comparing sounding curves, introduced by Habberjam (1976), was

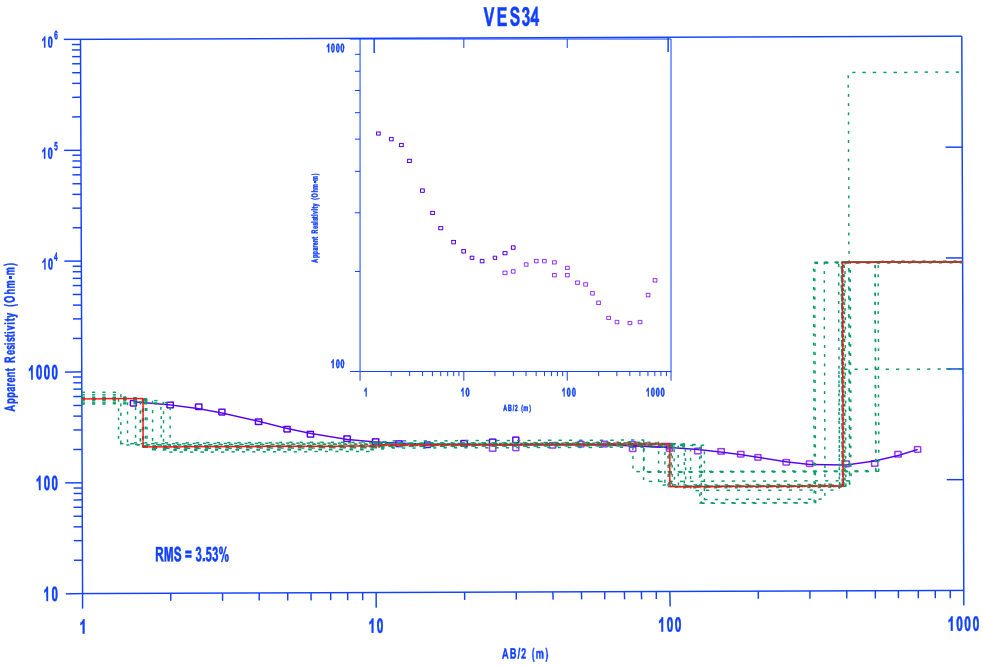

Fig. 2 VES 34, a typical sounding curve obtained in the investigated area. The best fit 1-D model and the corresponding equivalence models are also shown. The *inset figure* shows the raw data before applying the filter

utilized. The application of the method is in accordance with the calculations of the association factor, A_{ij}, for all the field curves using Eq. 2:

$$A_{ij} = \frac{1}{n+1} \sum_{r=1}^{r=n} \{\log p(r,i) - \log p(r,j)\}^2 \quad (2)$$

where

A_{ij} Association factor calculated for sounding curves conducted at sites i and j.
n Total number of sounding curves to be compared.
$p(r,i)$ Apparent resistivity measured at the site, i, using an electrode spacing of length r.
$p(r,j)$ Apparent resistivity measured at the site, j, using an electrode spacing of length r.

The calculated values of the association factor were utilized to construct the so-called likeness diagrams and likeness profiles. Based on a selected level for the likeness constant (C), it was possible to classify the field curves into several homogeneous groups. Two sounding curves were considered alike if the condition $A_{ij} < C$ is realized. The utilized value of the constant C was 0.01 which provided the most satisfactory classification. A typical likeness profile is provided in Fig. 3. This technique has been proved to be efficient in providing starting models as an input for the final 1-D inversion process of VES data.

Inversion of VES data

The inversion process aims to deduce the most probable parameters of the earth stratification; in particular, thickness and resistivity values. A computer automatic inversion program, Resix (Interpex 1998), was used for this purpose. The results of the quantitative interpretation were represented in four geoelectrical cross sections that extended in the W-E direction (i.e., perpendicular to the regional strike of the main tectonic features present in the area).

Resistivity cross section no. 1 This cross section consists of 20 sounding stations. It has a total length of about 1 km and extends within the coordinates: $X = 0.63$, $Y = 118$ km (VES 1) and $X = 161$, $Y = 118$ km (VES 20). These coordinates refer to the locally adopted coordination system (as shown in Fig. 1a). As can be seen in Fig. 4, four main electrical layers can be distinguished. The thin surface layer (less than 2 m of thickness) has a high resistivity values (more than 600 Ωm) and extends almost along the whole cross section. According to the local geology, this layer represents the upper part of the alluvium wadi sediments consisting mainly of dry sand.

The second layer is almost limited to the western part of the cross section (VES nos. 1, 2, and 4) and shows a relatively constant resistivity value of about 45 Ωm, where it has the thickness of about 70 m. This may indicate another part of the wadi sediments with high clayey contents.

The third layer represents the central part of the section and extends almost along the whole cross section. It has resistivity values within the range of 65 to 180 Ωm and showing a highly variable thickness (starting with about 100 m at western part (VES 4) and reaching its maximum value at the central part of the cross section (VES 7, 8, and 9) of about 450 m. This variation in thickness is almost identical at the eastern part of the cross section; it starts with 100 m at VES 19 and increases towards the central part of the section. This layer may correspond to the sandstone formation, locally known as the Rum sandstone group, consisting mainly of medium- to coarse-grained sandstone with contents of micaceous, ferrugineus sandstone.

The substratum is a highly resistive layer having the resistivity average value of about 450 Ωm. This layer indicates the upper part of the basement complex, composed mainly of medium- to coarse-grained granite.

Resistivity cross section 2 This cross section consists of 12 sounding stations and extends along a distance of 0.8 km, with

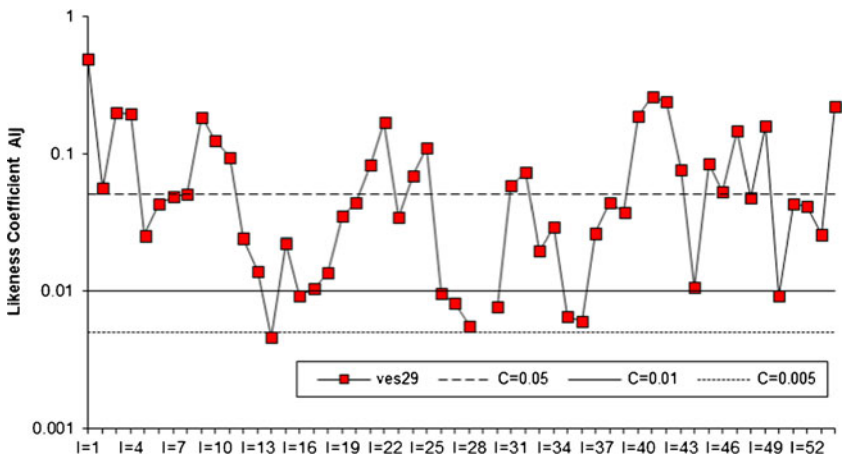

Fig. 3 A typical likeness profile obtained for the VES sounding stations conducted in the study area

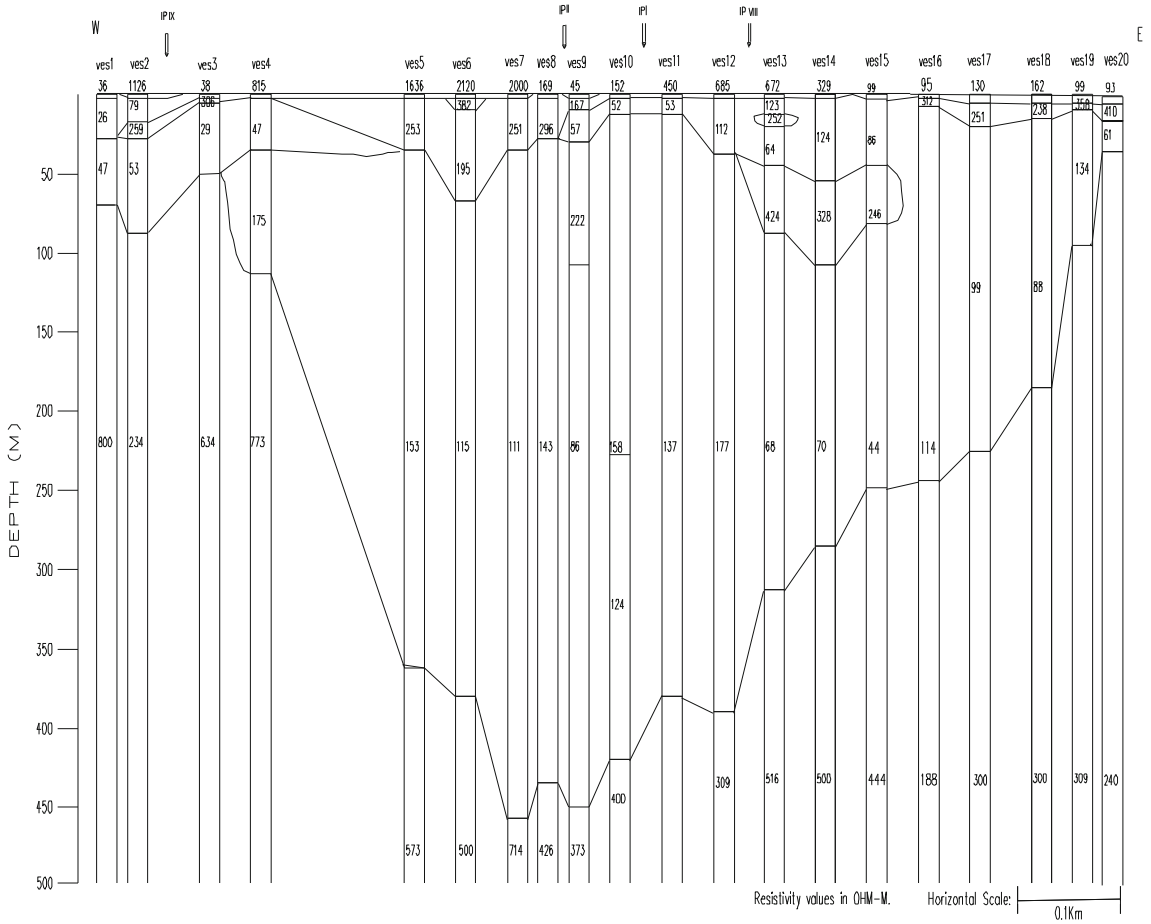

Fig. 4 Resistivity cross section 1—the vertical scale is the depth below the sounding station. All sounding stations are located at a flat area

the following starting-ending coordinates: (82, 99)—at Sounding station 21—and (163, 99), at VES 32. The electrical stratigraphy of the section shows the presence of four main layers (Fig. 5); the top layer is a thin resistive one which has a resistivity of more than 600 Ωm. It extends along the whole cross section and corresponds to the uppermost part of the alluvium sediments.

The second layer is an intermediate resistive one. It encompasses an average value of resistivity value of 250 Ωm. It indicates the lower part of wadi sediments. The relatively low resistivity value may be attributed to the presence of high amount of clayey materials.

The third layer is a conductive one with a uniform resistivity value of about 100 Ωm. It has a minimum thickness value at both western (147 m at VES 21) and eastern (74 m at VES 32) sides of the cross section, while maximum is at the central part (up to 310 m at VES 25). This variation in thickness is confirmed also in cross section 1. The resistive substratum holds the average resistivity value of almost 350 Ωm, indicating the upper granitic part of the basement complex.

Resistivity cross section 3 This cross section is the shortest one; it has a total length of about 0.4 km and is composed of eight sounding stations (Fig. 6). The electrical stratigraphy derived along this section is similar to those derived for the previous sections at their central and eastern parts; in particular, the resistive topmost layer has resistivity values that exceed 400 Ωm and thickness of less than 3 m.

The intermediate layer has a resistivity value of approximately 200 Ωm and has a relatively constant thickness of about 40 m. The central layer encompasses an average value of resistivity to be about 100 Ωm and an increasing thickness from about 20 m at the eastern part to about 310 m at the section's western end (VES 33). The uppermost part of the basement complex has a medium resistivity of almost 300 Ω m.

Resistivity cross section 4 The cross section extends along a line of about 1 km length. It consists of 14 sounding stations starting with VES 41 and ending with VES 54. Generally, this cross section shows geoelectrical stratification similar to that obtained for the previous cross sections (Fig. 7). The uppermost thin layer of the wadi sediments has a resistivity value of more than 500 Ωm. Its thickness does not exceed the 3 m.

The intermediate resistivity (an average of about 250 Ωm) layer extends along the whole cross section. The central part

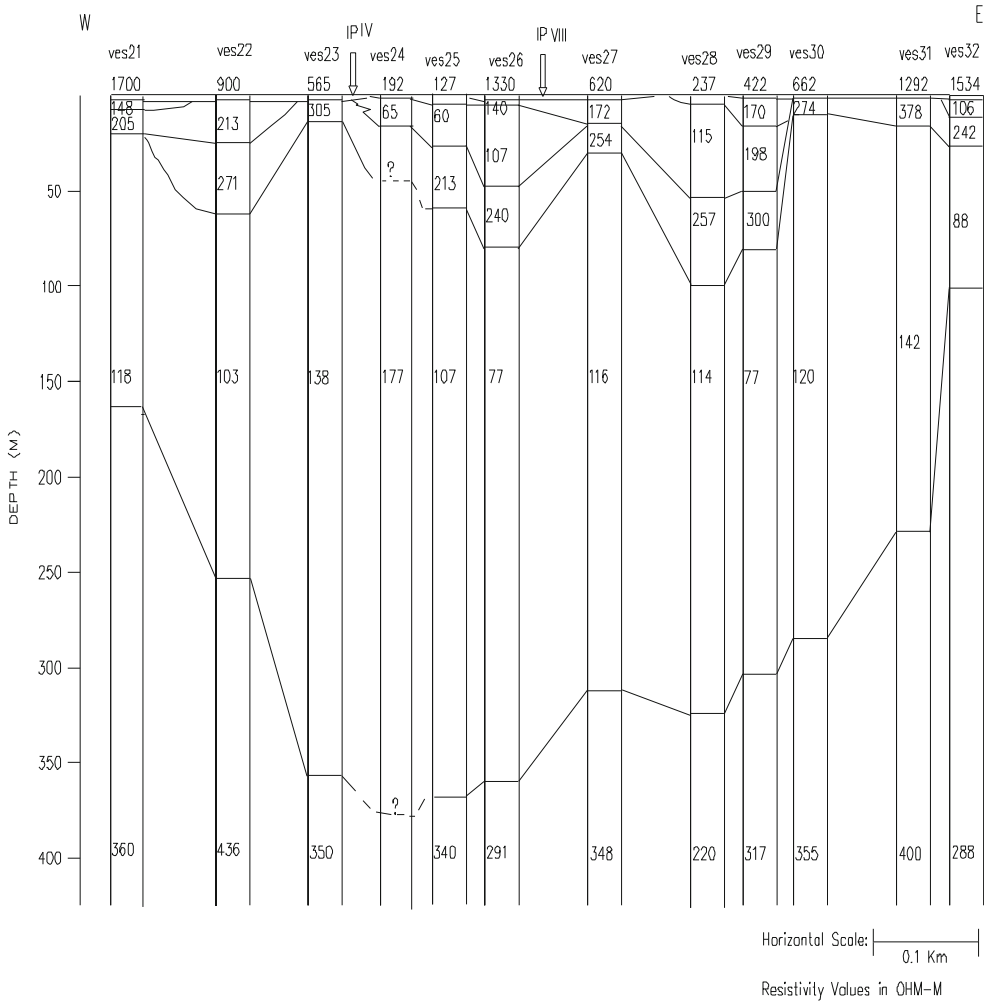

Fig. 5 Resistivity cross section 2—the vertical scale is the depth below the sounding station. All sounding stations are located at a flat area

of the section is composed of a thick layer with an average resistivity of about 100 Ωm. The variation in the thickness of this layer shows a similar behavior as it is in the previous cross sections. The resistive basement complex shows an average resistivity value of about 550 Ωm.

IP data

Processing

The software Statistica from StatSoft, Inc. has been used to carry out the statistical analysis of IP data. It has been noticed that resistivity values have a wide range starting from about 50 to about 1500 Ωm. However, about 98 % of the values are limited to the range of 100–1000 Ωm; this interval agrees well with resistivity values obtained in the VES interpretation. Resistivity values are centered about the value of 255 Ωm, while the metal factor values are centered about the value of 4 Mohs/m.

Two forms of data representation were utilized to display the measured apparent resistivity and metal factor values; in the first, the pseudosections representation is used. The approximate depth values in the pseudosections were assigned for the various depth levels of the pseudosections ($N=1$, 2 etc.) taking in consideration the definitions of depth of investigation for the dipole configuration provided by Roy (1972) and the definition provided by Barker (1989).

The depth map is the other method used for IP data representation. The construction of the depth maps was done utilizing the level values ($N=1$, $N=2$, etc.). This type of representation is efficient in displaying the variations in the characteristics of the investigated medium at certain depth and the continuity of the existed structures in the vertical direction.

Interpretation

IP profiles could be classified into three different groups according to their orientation with respect to the general strike direction in the area. These are profiles directed to NW-SE, profiles directed to SW-NE, and profiles perpendicular and

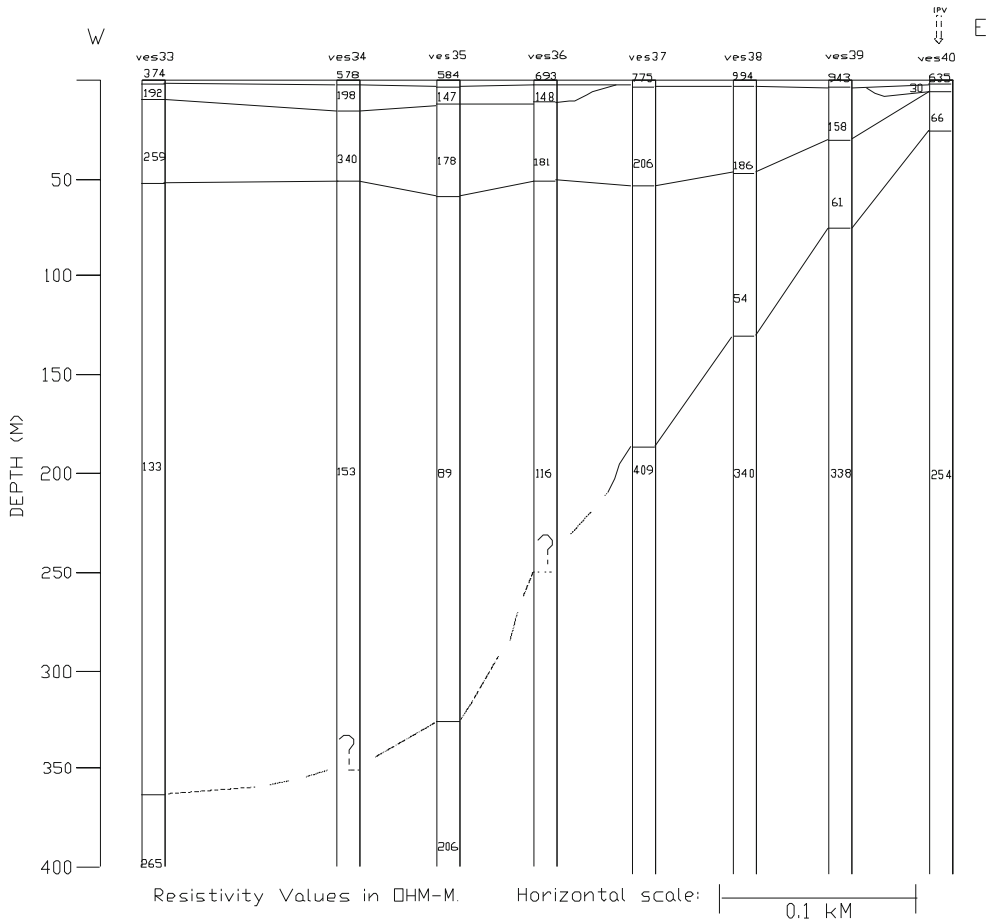

Figure 6 Resistivity cross section 3—the vertical scale is the depth below the sounding station. All sounding stations are located at a flat area

parallel to the strike. The interpretation of these profiles is given below:

Resistivity pseudosections-NW-SE profiles This group includes three profiles, these are profiles II, III, and I. Profile I (as shown in Fig. 8) extends along a distance of about 1.5 km and it has the NW-SE trends. The pseudo section of the apparent resistivity can be interpreted qualitatively to be composed of three main blocks; the first block is a resistive one that has resistivity values that exceed 125 Ωm. The boundary of this block can be defined by the coordinates of $X = 0.25$ to 0.6 km and extend along the whole depth range of the pseudosection. The resistivity values of this block increase towards the NW direction.

The second block occupies the central part of the section and it has low resistivity values (less than 125 Ωm). The extension of the block is limited within the X range of 0.6 to 1.45 km. Vertically, this block extends along the whole depth levels of the pseudosection.

The third block is a resistive one; it has the resistivity values that exceed the 125 Ωm. The boundary of this block is detected at the X range value of 1.45 to 1.7 km.

Profile II (Fig. 9) shows similar characteristics of the previous profile. It has a length of 1.7 km and can be qualitatively interpreted to be composed of three blocks. The first block is composed of resistive formation that has a resistivity value exceeding the 125 Ωm. It is limited by the X range of 0.24 to 0.74, its resistivity increases rapidly towards the NW direction.

The central part of the section is composed of a relatively low resistive block of less than 125 Ωm. This block is limited in the X range of 0.64 and 1.44 km. Vertically, it has the same resistivity trend over the whole depth levels.

The SE resistive part of the section, it has resistivity values of more than 125 Ωm. It extends starting from the X value of 1.44 km. The resistivity shows a gradual increase towards the SE direction.

Profile III extends along a distance of 1.6 km (Fig. 10). The NW resistive block extends along the $X = 0.3$ to 0.7 km, it has resistivity values of more than 125 Ωm. It shows a similar behavior to its equivalence in the previously interpreted profiles. The conductive central block extends along an X range of 0.7 to 1.4 km. Resistivity values are less than 125 Ωm. The resistive SE block extends along X range of 1.4 to 1.6 km. Resistivity values exceed 125 Ωm.

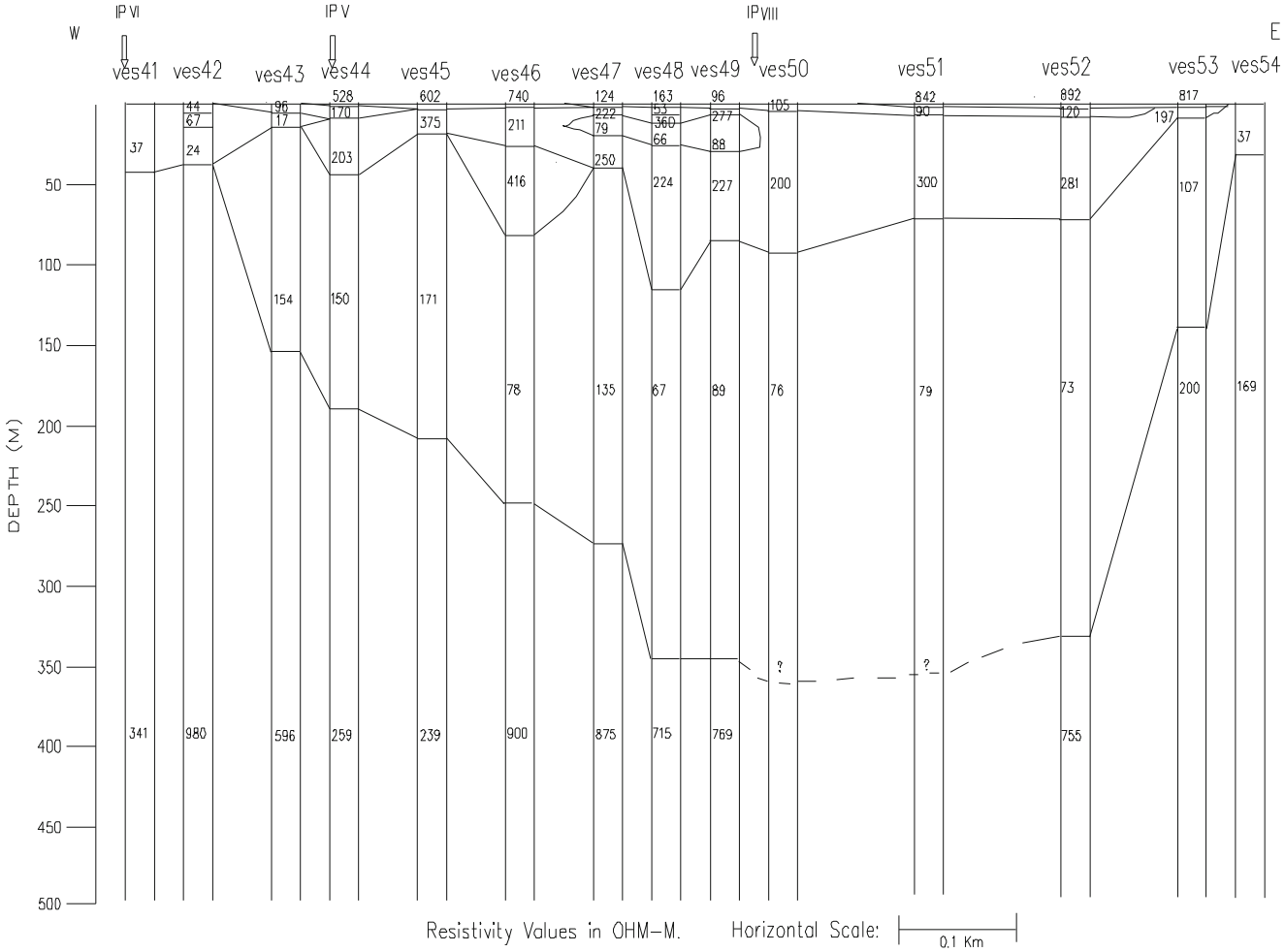

Fig. 7 Resistivity cross section 4—the vertical scale is the depth below the sounding station. All sounding stations are located at a flat area

SW-NE profiles This group includes the profiles IV, V, and VI. In the following section, description of these is given.

Profile IV (Fig. 11) extends along a distance of about 1.8 km; it shows also the presence of three main blocks. The resistive SW block (resistivity >125 Ωm) which extends along the *X* range of 0.5 to 0.8 km. Its resistivity increases with depth.

The central part has a relatively low resistive block (less than 125 Ωm) and it is limited by the *X* range of 0.9 to 1.55 km. It extends vertically along the whole depth levels. The NE resistive part starts at the *X* value of 1.55 km. Its resistivity increases in the NE trend.

Profile V extends along a distance of about 1.6 km (Fig. 12). The SW resistive part of this profile starts at an *X* value of 0.3 and extends to 0.6 km and its resistivity increases towards the SW direction. The central part is dominated by a low resistive block. This block extends along the *X* range of 0.6 to 1.36 km. The NE part starts at $X = 1.36$ having the resistivity value of 125 Ωm which increases to more than 250 Ωm at the extreme NE part of the pseudo section.

In profile VI (Fig. 13), the SW part is a resistive block that extends along an *X* range of 0.3 to 0.8 km; its resistivity increases rapidly towards the SW direction. The central part of the pseudo section is occupied by a low resistivity block (less than 125 Ωm) and extends along the *X* range of 0.7 to 1.6 km. The resistive block at the NE part is not shown by this section; this may be attributed to the relatively short length of the profile. However, the general behavior of the resistivity and extensions of the detected blocks are also maintained along this profile.

Profiles perpendicular and parallel to the strike This group contains three profiles, of which two are parallel to the strike direction (profiles VIII and IX), while the third one is perpendicular to the strike direction (profile VII).

Profile VII (Fig. 14) has a total length of 1.5 km and is oriented in the W-E direction. Along this profile, a resistive block appears at the western part of the section that has resistivity values of more than 125 Ωm. It starts at an *X* value of 0.1 and extends to an *X* value of 0.9 km.

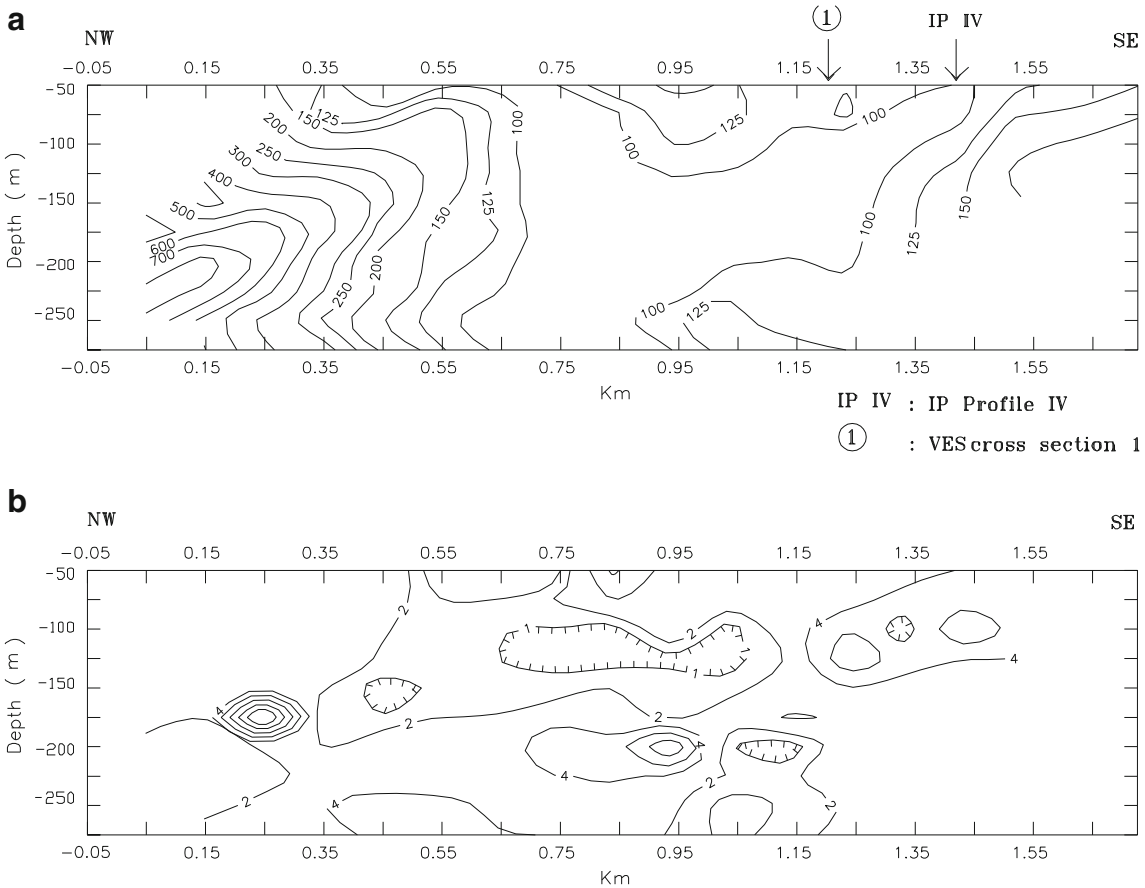

Fig. 8 Induced polarization pseudosections of profile I. **a** Apparent resistivity in Ohm meters and **b** metal factor in mohs per meter

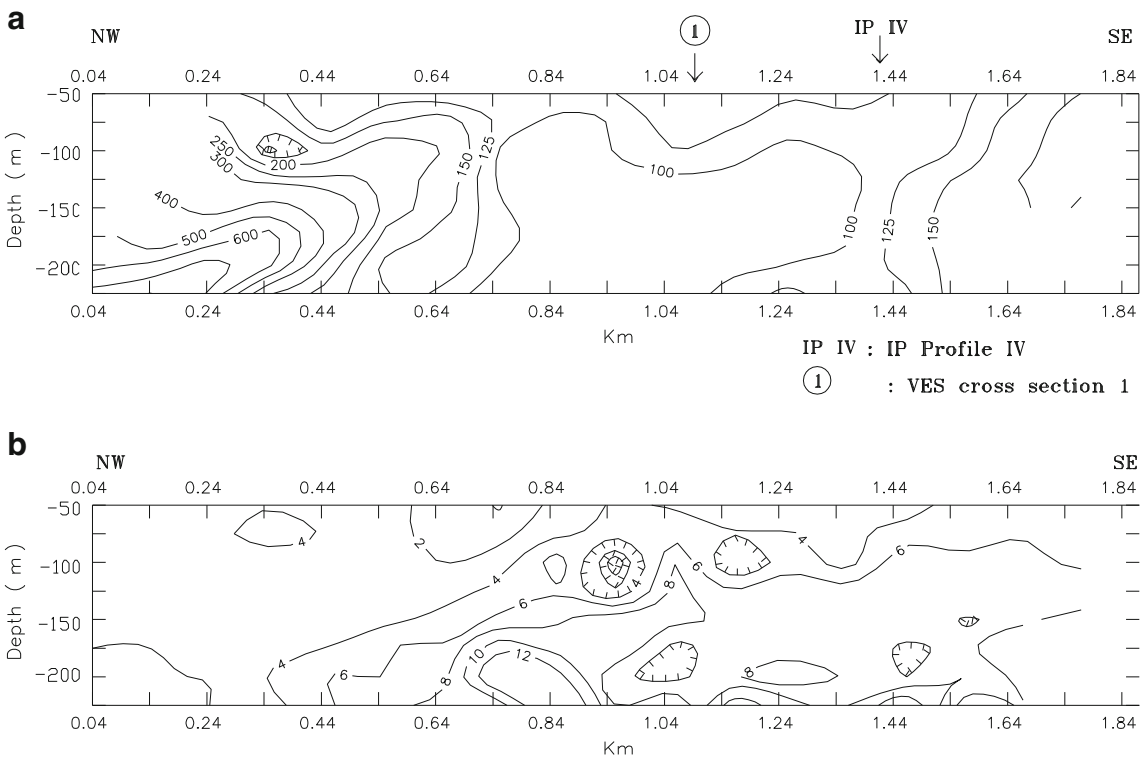

Fig. 9 Induced polarization pseudosections of profile II. **a** Apparent resistivity in Ohm meters and **b** metal factor in mohs per meter

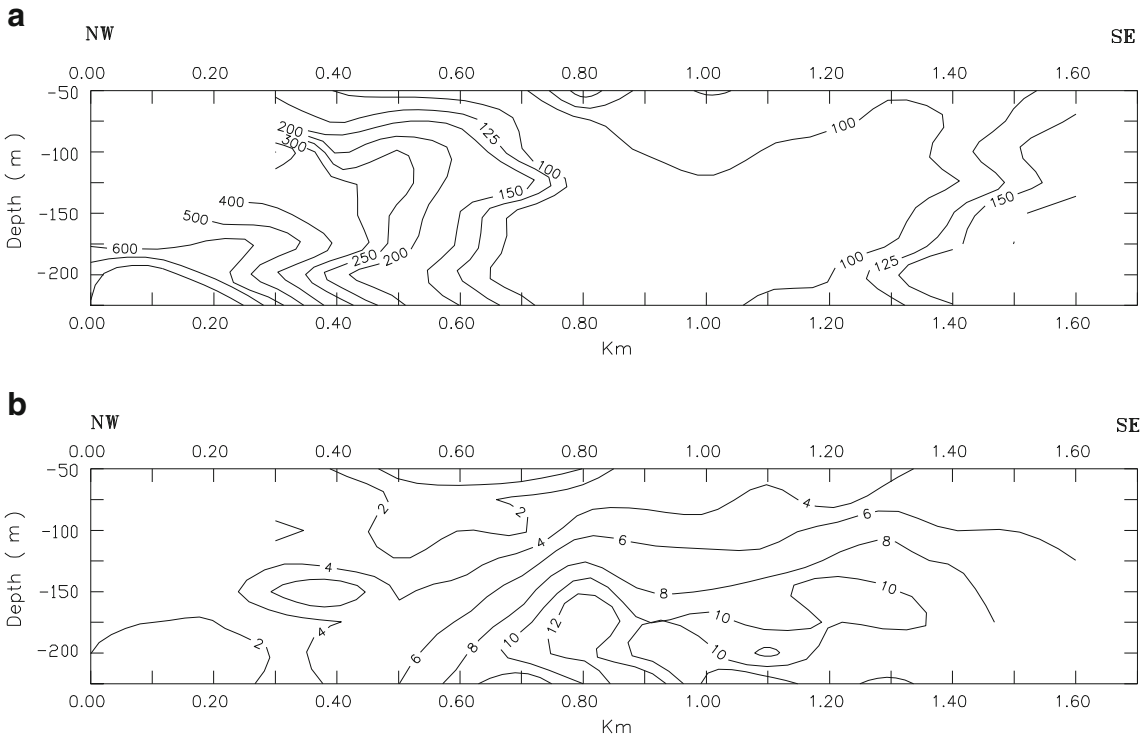

Fig. 10 Induced polarization pseudosections of profile III. **a** Apparent resistivity in Ohm meters and **b** metal factor in mohs per meter

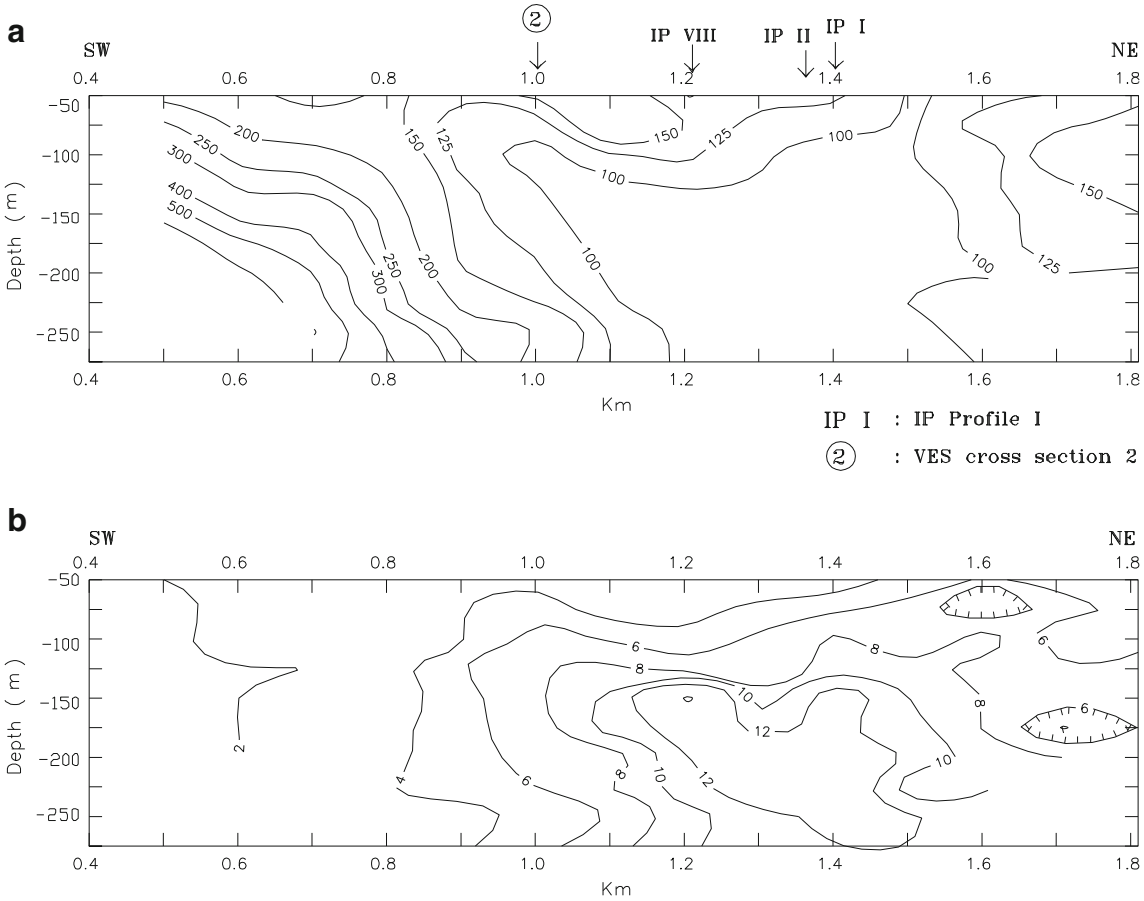

Fig. 11 Induced polarization pseudosections of profile IV. **a** Apparent resistivity in Ohm meters and **b** metal factor in mohs per meter

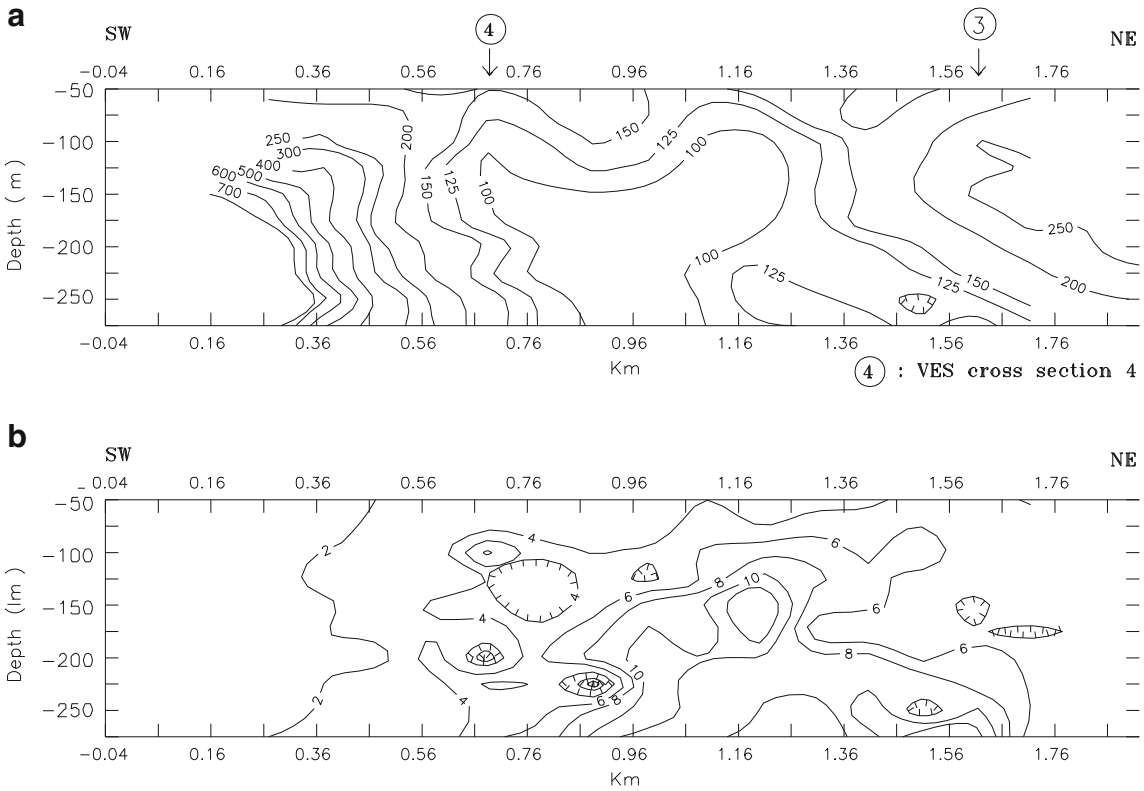

Fig. 12 Induced polarization pseudosections of profile V. **a** Apparent resistivity in Ohm meters and **b** metal factor in mohs per meter

A second block is the central one; it extends within the *X* range of 0.9 to 1.5 km. In the vertical direction, it reaches a depth of about 150 m. The increment in the resistivity of this block can be noticed at greater depths (about 400 Ωm at

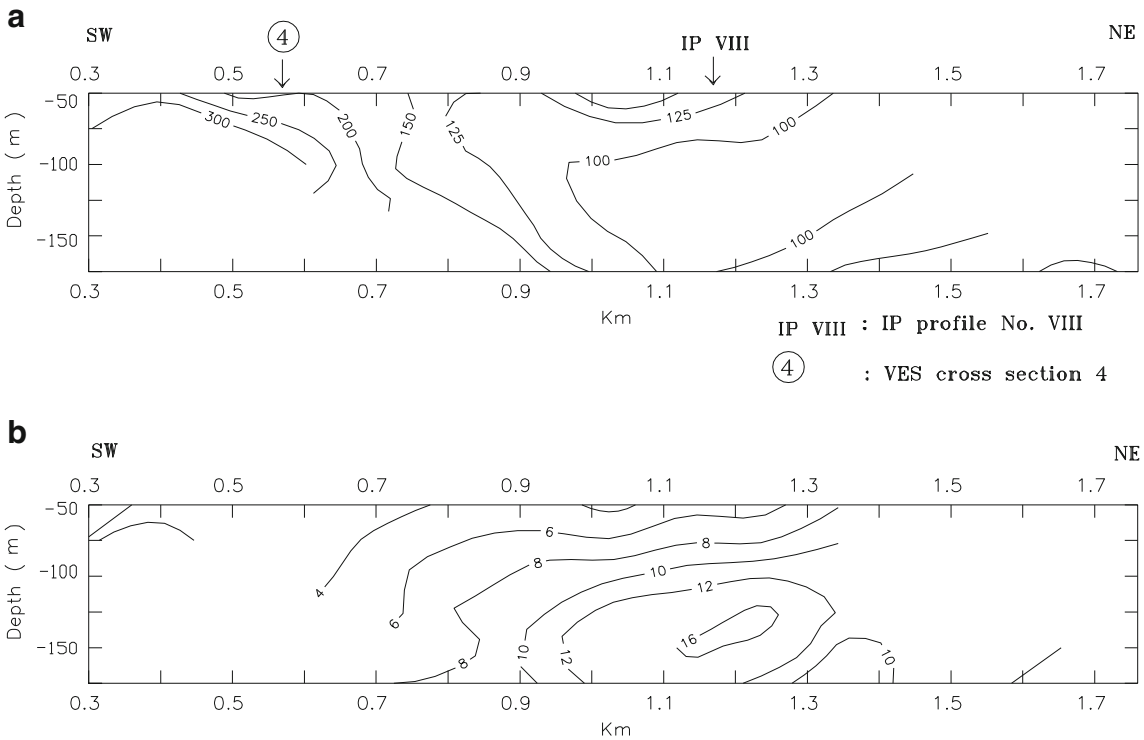

Fig. 13 Induced polarization pseudosections of profile VI. **a** Apparent resistivity in Ohm meters and **b** metal factor in mohs per meter

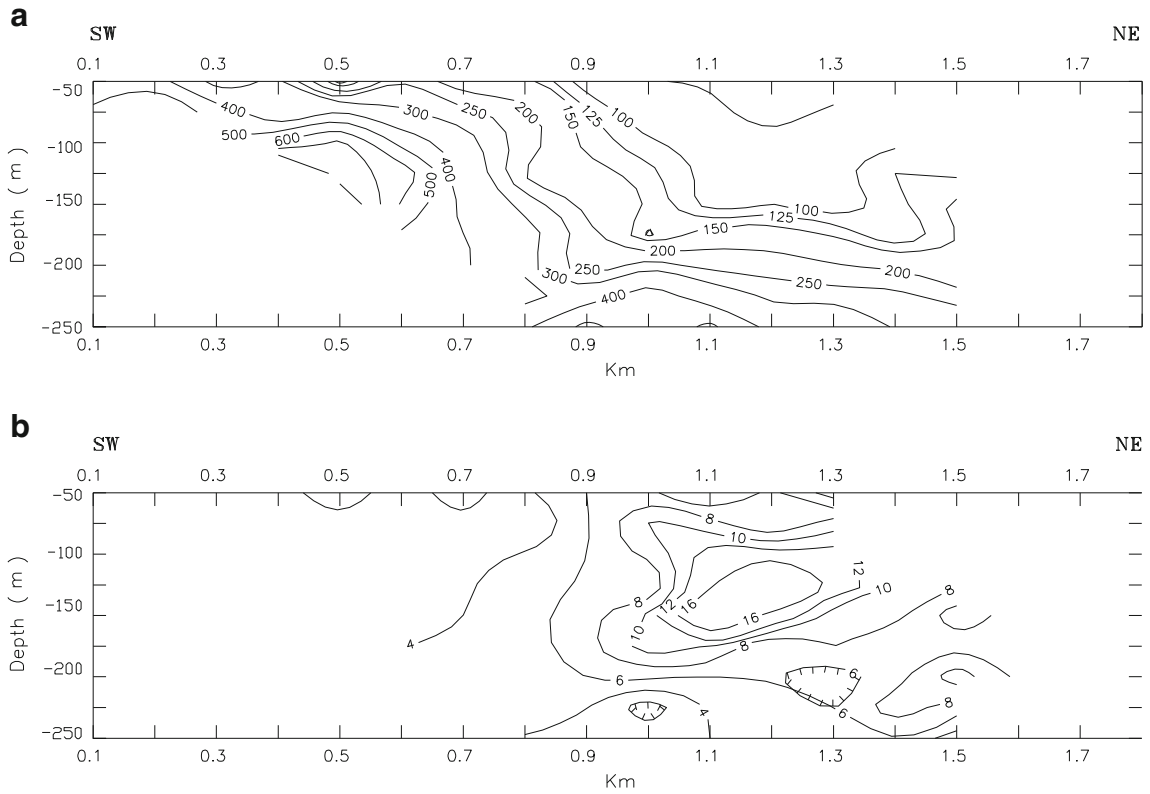

Fig. 14 Induced polarization pseudosections of profile VII. **a** Apparent resistivity in Ohm meters and **b** metal factor in mohs per meter

maximum level of depth). The eastern part of the pseudo section, starts at an *X* value 1.4 km; it is a resistive one with the resistivity increases from 125 to more than 200 Ωm towards the extreme eastern part.

Profile VIII (Fig. 15) is conducted at the central part of area and extends along 2.5 km in a parallel direction to the strike. The qualitative interpretation shows no great variations in the resistivity values. Generally, these are less than 200 Ωm and extend along the whole levels of depths.

Profile IX (Fig. 16) extends along a distance of about 2.0 km and has the SW-NE trend. This profile shows mainly resistive blocks. It starts with a resistive layer that extends along the whole length of the profile; while vertically, it extends to a depth of about 75 m. It has an average resistivity of about 150 Ωm. The deeper layer has resistivity increases with depth starting at a value of about 250 Ωm at a depth of 75 m and increases to more than 700 Ωm at a depth of 125 m.

MF pseudo sections-NW-SE profiles Generally, it can be said that the values of the metal factor in these pseudosections increase with depth; this behavior can be seen in the major parts of the pseudosection. The MF values increase from about 2 mohs/s at surface levels to more than 8 mohs/m at depths exceeding 150 m (see Figs. 8b, 9b, and 10b). However, minimum values which are found at depth can be indicated in profile I. It lies at the depth of about 200 m and centered at *X*= 1.1 km. The value is less than 2 mohs/m. Similar values can also be seen in profile II. These are found at a depth of about 200 m and centered at *X* values of 1.04 and 1.44 km. it has a value of 6 mohs/m. A maximum value (more than 10 mohs/m) is also shown by profile I at a depth of 175 m. It is centered at an *X* value of 0.25 km.

SW-NE profiles Several observations can be made regarding the MF pseudosections. In general, it can be indicated that the MF maximum values correspond to those of the lower resistivity zones in the resistivity pseudosections, and vice versa. It can be noticed also that the maximum values of MF are concentrated at the central part of the study area whereas these values decrease towards the SW and NE directions. The blocks of low MF values correspond, in fact, to the SW and NE resistive blocks (see Figs. 10, 11 and 13).

Several minimum values of the MF can be indicated: in profile IV, the minimum values are limited to the SW block and along the *X* range of 1.5 to 1.8 km at several depth levels (Fig. 11). In profile V (Fig. 12), at an *X* range of 0.66 to 0.86 that extends to the depth of almost 200 m and at an *X* range of 0.8 to 0.9 km extends at a depth level of about 250 m. In profile VI (Fig. 13), the minimum values are restricted to the surface depth levels.

Profiles parallel and perpendicular to the strike Figure 14 (profile VII), which is perpendicular to the strike direction,

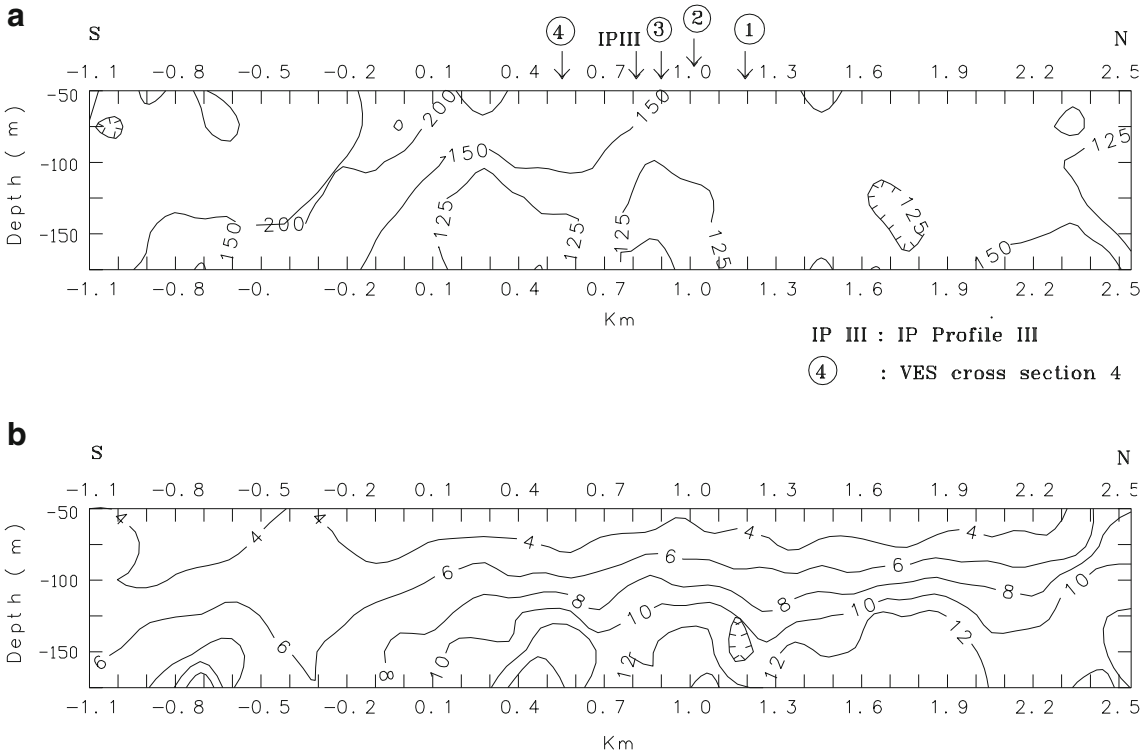

Fig. 15 Induced polarization pseudosections of profile VIII. **a** Apparent resistivity in Ohm meters and **b** metal factor in mohs per meter

shows that the high MF values are concentrated at the central part of the cross section, where the minimum values are concentrated at eastern part of the section. The MF values are in the range of 6–16 mohs/m.

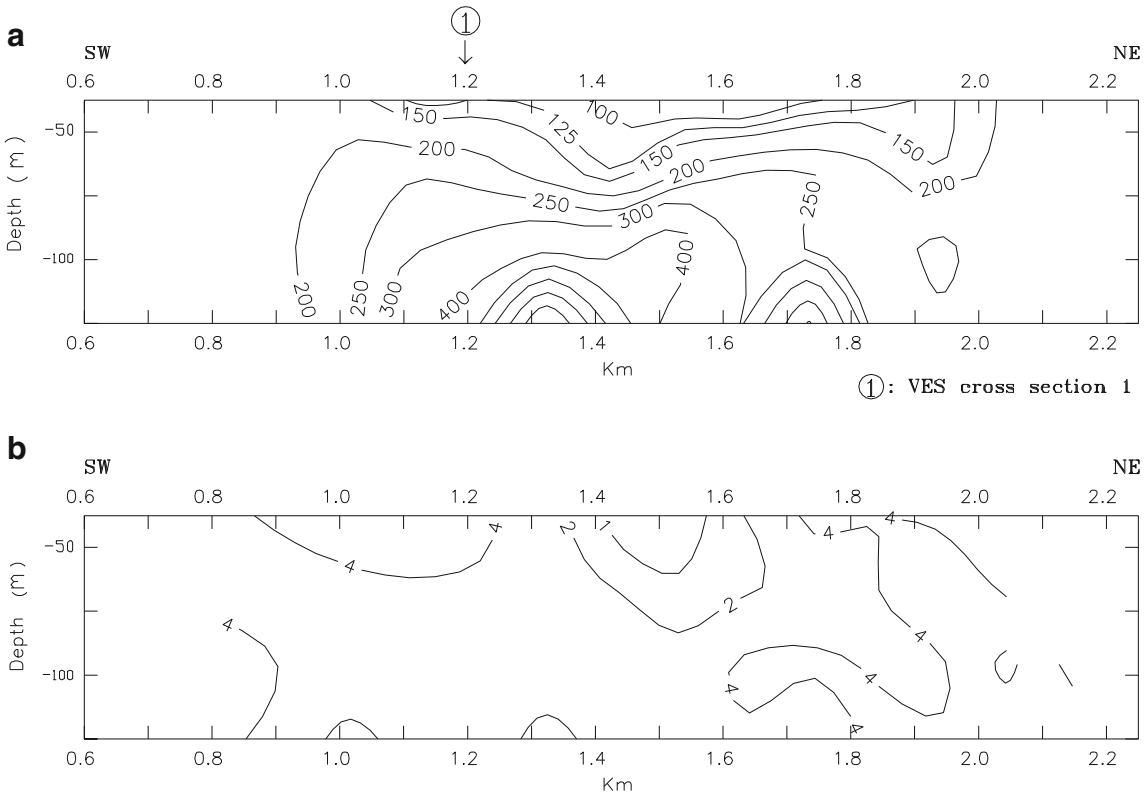

Fig. 16 Induced polarization pseudosections of profile IX. **a** Apparent resistivity in Ohm meters and **b** metal factor in mohs per meter

In the profiles conducted in a parallel direction to the strike, it could be noticed that profile VIII (Fig. 15), conducted at the central part of the area, is characterized by horizontal extension of contour lines with a vertical increasing of the MF values. These are in the range of 4 to 14 mohs/m. Profile IX (Fig. 16), has low variations in the MF values; these are in the range of 1 to 4 with the small values restricted to the surface levels.

Apparent resistivity depth maps Depth level $N=1$ (Fig. 17) is dominated by relatively low resistivity values (100 to 250 Ω m). It also emphasizes the increasing resistivity trend towards the eastern and the western sides of the study area. The lower resistivity values are concentrated at the central part of the area (≤125 Ωm). However, the resistive block is seemed to be limited within the following coordinates: $X=0.5$ to 1.3 km and $Y=1.1$ to 2 km.

At a depth level of $N=2$ (Fig. 18), the area seems to be divided into three different zones according to their resistivity values: the first block is a resistive one (resistivity values of more than 125 Ωm) which is limited by the X coordinates of 0.2 to 1.1 km and the Y coordinates of 0.2 to 1.6 km. The central part of the area is occupied by a low resistivity formation (resistivity values of less than 125 Ωm m) and extends within the coordinates $X=0.8$ to 1.4 km and $Y=0.2$ to 1.6 km. The eastern part of the area is composed of another resistive formation of values more than 125 Ωm. This block starts at the coordinates of $X=1.4$ to 1.75 km and $Y=0.2$ to 1.6 km. An interesting feature that can be seen at this level is the graben structure already indicated by both the VES and the IP pseudo section interpretations.

At a depth level of $N=3$ (Fig. 19), a similar situation to that seen at depth level $N=2$ can be observed. Firstly, the boundaries of the westerly resistive block are detected at the following coordinates: $X=0$ to 0.8 km and $Y=0.2$ to 1.6 km. The central low resistivity block lies within the coordinates of $X=0.8$ to 1.2 km and $Y=0$ to 1 km. The resistivity of the block is ≤125 Ωm. The eastern resistive block (resistivity >125 Ωm) starts at the coordinates of $X=1.4$ to 1.8 km.

At a depth level of $N=4$ (Fig. 20a), the similar interpretation to that provided for the previous two levels can be made. However, the graben boundaries at this level are detected at the coordinates $X=0.1$ to 0.8 km and $Y=0.8$ to 1.6 km.

At a depth level of $N=5$ (Fig. 21), the same characteristics of the previously interpreted levels exist, except that the western resistive block has not been detected very clearly. The coordinates of the graben structure are determined at $X=0$ to 0.8 km and $Y=0.7$ to 1.7 km, whereas the central low resistivity block extends from the coordinates of $X=0.6$ and $Y=0.5$ to 0.6 Km.

MF depth maps At a level of $N=1$ (Fig. 17b), the variation in MF values is limited (values are in the range of 2–6 mohs/m), this may indicate the surface formations in the area.

The depth level of $N=2$ (Fig. 18b) has values in the range of 1 to 12 extending along the whole area. By comparing it to the resistivity depth map at this level, a confirmation is obtained that high MF values correspond to low resistivity values and vice versa; this was also obtained from the interpretation of the IP pseudo sections. Other minimum value to be indicated (2 mohs/m) lies at the coordinates $X=0.4$ to 0.9 and $Y=0.9$ to 1.5 km.

At a depth level of $N=3$ (Fig. 19b), the obtained MF behavior corresponds very well to that of the apparent resistivity at the same level. To be also indicated are the minimum values (less than 6) at the coordinates of $X=0.8$ to 1.2 and the $Y=0$ to 1. Generally, the values obtained are in the range of 2 to 12 mohs/m.

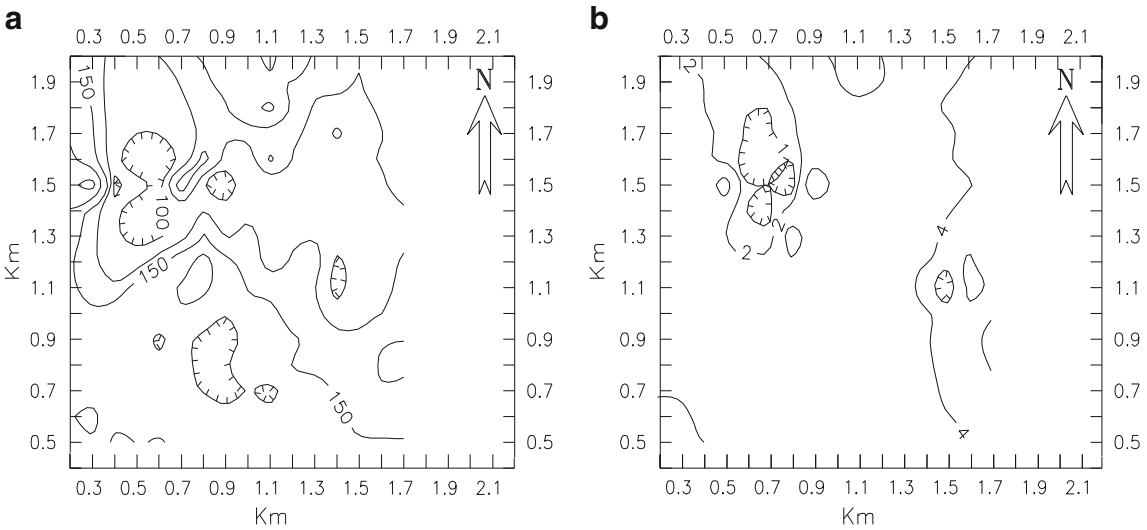

Fig. 17 Induced polarization depth maps at level $N=1$. **a** Apparent resistivity in Ohm meters and **b** metal factor in mohs per meter

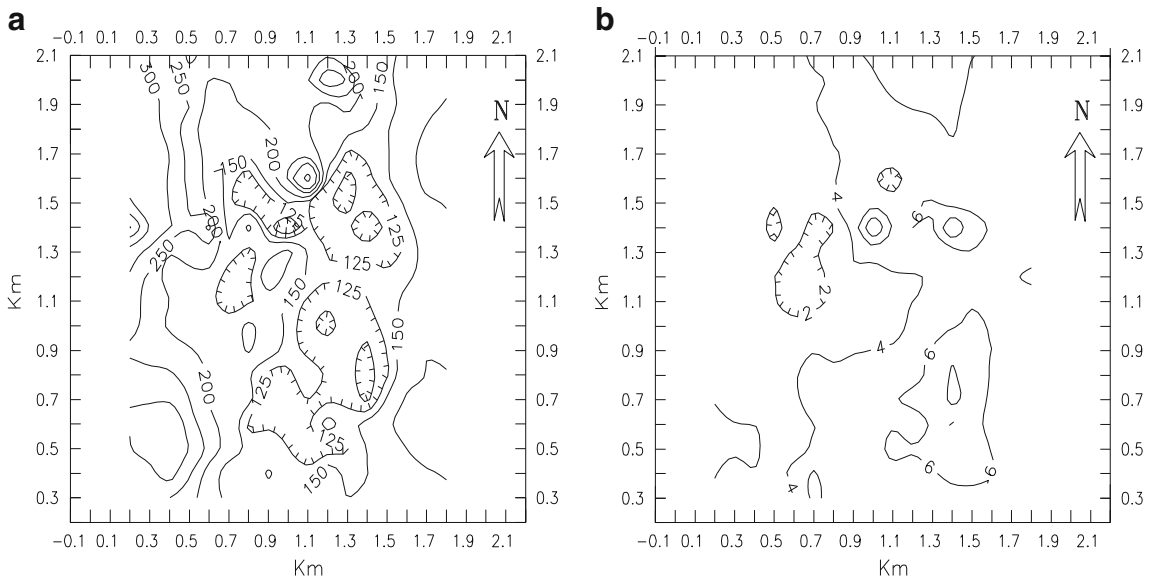

Fig. 18 Induced polarization depth maps at level $N=2$. **a** Apparent resistivity in Ohm meters. **b** metal factor in mohs per meter

At a depth level of $N=4$ (Fig. 20b), values in the range of 2–12 are also obtained where minimum values can be indicated at the western parts of the area and the maximums at the central part. At a depth level of $N=5$ (Fig. 21b), the minimum values correspond to the western and eastern parts of the area, where the maximums are concentrated at the central part (>8).

Discussion and conclusion

The integrated use of VES and IP methods has been applied in the present study to determine the electrical properties stratification in the study area. The application of qualitative interpretation of the IP measurements, specifically MF and resistivity, for structural investigation has been also evaluated.

The inversion of the VES curves was done taking in consideration the outcomes of the qualitative information derived from the IP measurements and the classification of the VES field curves into several homogeneous groups, each of which is represented by one model (within the chosen limits of precision). This procedure was effective in reducing the effect of the equivalence problem.

The study has used Schlumberger VES technique instead of profiling using WennerSchlumberger because of the fact that the VES technique provides an image of the subsurface forming horizontal layers. It is considered as the customary rule of thumb for claiming the investigation's depth is of the

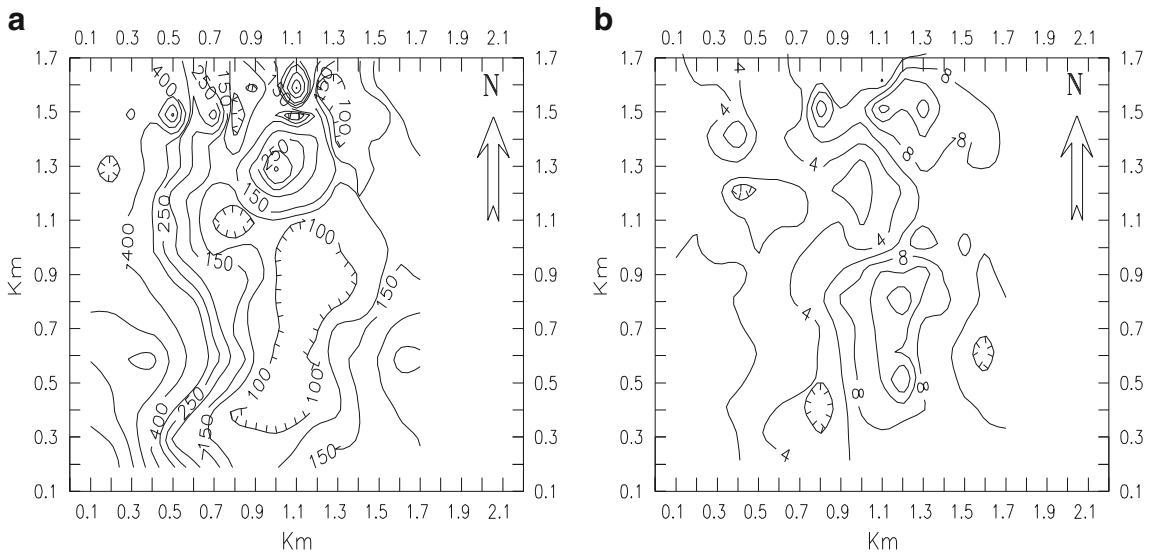

Fig. 19 Induced polarization depth maps at level $N=3$. **a** Apparent resistivity in Ohm meters and **b** metal factor in mohs per meter

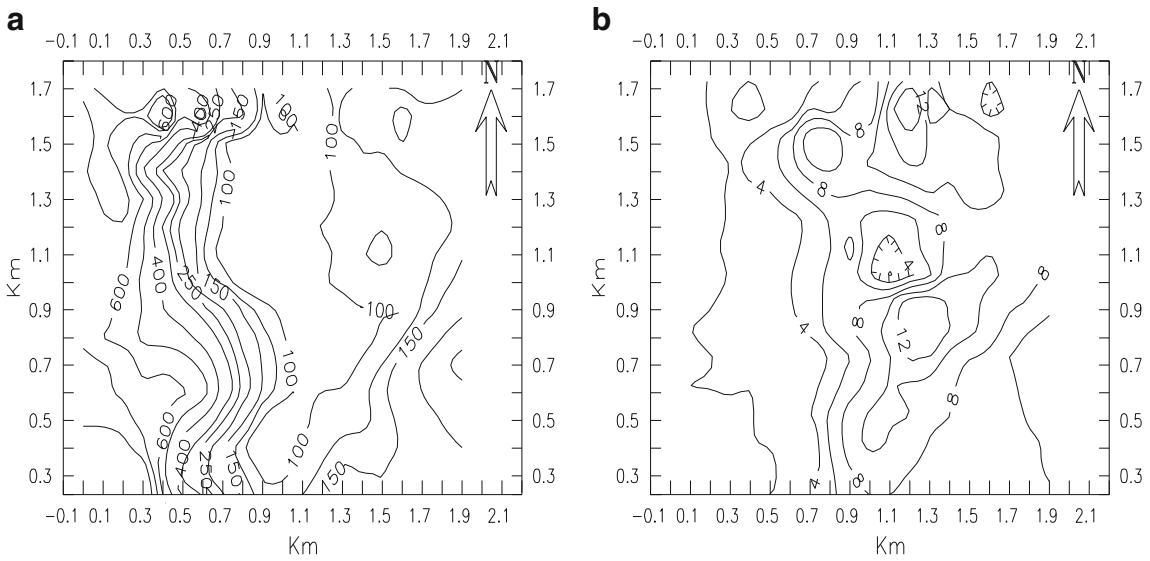

Fig. 20 Induced polarization depth maps at level $N = 4$. **a** Apparent resistivity in Ohm meters and **b** metal factor in mohs per meter

order of 0.1–0.3 times the length of line AB. Furthermore, this depth depends mainly on the layering type which has been deployed. On the other hand, in the conventional WennerSchlumberger electrical sounding, the transmission electrodes of A and B are sequentially backed off from each other while considering new readings for ensuring the increment in the investigation's depth (Bernard 2003). The lengths of MN and AB are controlled completely by the operator. It is due to the fact that the four electrodes as well as their wires are considered to be independent. It has been revealed that the time required for moving from one position to another gets longer for carrying out deep investigations; thus, it appears to be essential that significant time is provided for stacking the signal in order to enhance reading quality or making the reading possible.

The present study shows that the traditional VES technique can still be used in areas where little direct geological data are available to provide valuable information about subsurface structural investigated features. This is particularly valid when VES data processing and interpretation are supported by effective qualitative techniques, such as the association factor. In addition, the cross sections constructed on the base of quantitative VES data interpretation provided the approximate boundaries of a graben structure found in the area.

Furthermore, the results of the IP technique proved to be indicative. The apparent resistivity pseudosections and maps provided an image of the subsurface and mapped the approximate boundaries of the main structural feature. This has been confirmed by the MF values where an expected inverse relationship can be noticed, i.e., high resistivity values correspond to formations with low MF values and vice versa (e.g., see Figs. 12, 13, and 14). This explains the presence of lower MF values at the western and eastern blocks (resistive) of the graben structure compared to its central part which has low MF values; this part is mainly composed of conductive sedimentary formations that extend to large depth ranges. This might be an indication on a subsidence tectonic activity that led to the formation of this structure.

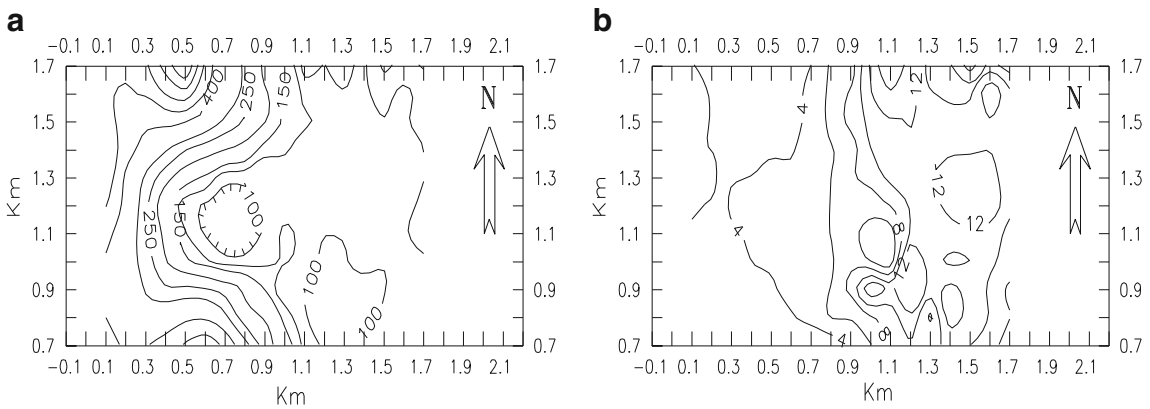

Fig. 21 Induced polarization depth maps at level $N = 5$. **a** Apparent resistivity in Ohm meters and **b** Metal factor in mohs per meter

The induce polarization, i.e., IP has been deployed for exploring the ore bodies, mainly disseminated sulfides. It is found that the deployment of induced polarization in engineering and geotechnical applications has become limited and it is being used widely for the exploration of groundwater. It is due to the fact that the studies related to groundwater exploration are associated with time domain.

By comparing the results obtained at the stations of intersections between the VES cross sections and the IP apparent resistivity and MF pseudosections, a fair constrain on the quality of the derived tectonic model could be noticed.

The findings and results of the study have shown that the technique of VES appears to be suitable and appropriate for the areas in which there is the availability of little direct geological data. It is due to the fact that it will assist in providing useful and adequate information related to investigated features of subsurface structure.

In conclusion, despite the lack of direct geological information available about the investigated area, the integrated use of quantitative interpretation of the VES sounding stations and the qualitative interpretation of IP data proved to be efficient in mapping structural features. With a reasonable accuracy, it was possible to map the vertical and lateral extensions of a graben structure present in the area. Still, however, other direct geological information (boreholes) is needed to optimize the derived tectonic model.

Acknowledgments The authors extend their appreciation to the Deanship of Scientific Research at King Saud University for funding this work through research group no. RG 1435-008.

References

Abdelhamid G (1990) The geology of Jabal Um Ishrin Area (Wadi Rum), National Resources Authority (Jordan), Bulletin 14, Map sheet No. 3049 II

Adepelumi AA, Yi MJ, Kim JH, Ako BD, Son JS (2006) Integration of surface geophysical methods for fracture detection in crystalline bedrocks of southwestern Nigeria. Hydrogeol J 14:1289

Barker RD (1989) Depth of investigation of collinear symmetrical four-electrode arrays. Geophysics 54:1031

Bender F (1974) Geology of Jordan. Gerbruder Borntraeger, Berlin, p 159

Bernard J (2003) Short note on the depth of investigation of electrical methods, heritage geophysics, retrieved from http://www.heritagegeophysics.com/papers/Depth_of_investigation.pdf

Ghosh DP (1971) The application of linear filtered theory to the direct interpretation of geological resistivity sounding measurement. Geophys Prospect 19:196

Habberjam GM (1976) The comparison of sounding results and their interpretation in the absence of borehole control. Geoexploration 14:220

Interpex Limited (1998) Resix scientific software, Golden, CO 80402, USA

Marshall D, Madden T (1959) Induced polarization, a study of its causes. Geophysics 24:803

Nicolas OM, Keller GR (2007) An integrated geophysical study of the northern Kenya rift. J Afr Earth Sci 48:85

Roy A (1972) Depth of investigation in Wenner, three-electrode and dipole-dipole DC resistivity methods. Geophys Prospect 20:332

Simiyu SM, Keller GR (1997) Integrated geophysical analysis of the East African Plateau from gravity anomalies and recent seismic studies. Tectonophysics 278:293

Sumner JS (1976) Principles of induced polarization for geophysical exploration, Elsevier scientific publishing company, ISBN 0-444-41481-9, p. 277